

The Streaming Batch Model for Efficient and Fault-Tolerant Heterogeneous Execution

Frank Sifei Luan^{1*} Ron Yifeng Wang^{1*} Yile Gu² Ziming Mao¹ Charlotte Lin¹ Amog Kamsetty^{1,3}
Hao Chen³ Cheng Su³ Balaji Veeramani³ Scott Lee³ SangBin Cho³ Clark Zinzow³
Eric Liang^{1,3} Ion Stoica^{1,3} Stephanie Wang^{2,3}

¹UC Berkeley ²University of Washington ³Anyscale

Abstract

While ML model training and inference are both GPU-intensive, CPU-based data processing is often the bottleneck. Distributed data processing systems based on the batch or stream processing models assume homogeneous resource requirements. They excel at CPU-based computation but either under-utilize heterogeneous resources or impose high overheads on failure and reconfiguration.

We introduce the *streaming batch* model, a hybrid of batch and streaming that enables efficient and fault-tolerant heterogeneous execution. The key idea is to use *partitions* as the unit of execution to achieve elasticity, but to allow partitions to be dynamically created and streamed between heterogeneous operators for memory-efficient pipelining. We present Ray Data, a streaming batch system that improves throughput on heterogeneous batch inference pipelines by 2.5–12× compared to traditional batch and stream processing systems. By leveraging heterogeneous clusters, Ray Data improves training throughput for multimodal models such as Stable Diffusion by 31% compared to single-node ML data loaders.

1 Introduction

Data processing is critical to machine learning (ML) applications. While ML workloads are known to be GPU-intensive, they also require significant I/O and CPU to load, preprocess, and move data to the GPU. Indeed, *CPU-based preprocessing is often the bottleneck* in both training [28] and batch inference [20]. Meanwhile, as ML models evolve, the data processing functionality required has also become more *diverse*, spanning many data modalities such as text, image, and video. These new workloads introduce complex transformations and resource requirements [16, 30, 38]. As ML models have grown larger in scale, there is also a critical need to *scale* the data processing alongside the ML workload.

At first glance, such applications seem simple to scale: both distributed training and batch inference can be expressed as dataflow graphs (Figure 1) where each node is an *operator* that executes a transform over its incoming data. The data

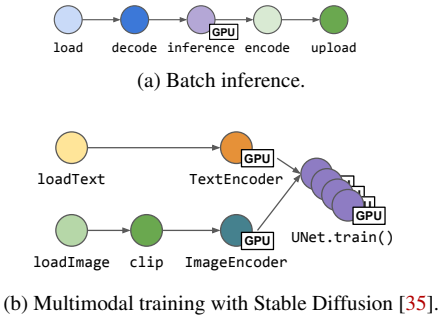


Figure 1: Logical dataflow graphs representing heterogeneous ML applications. (a) A pipeline for video or image generation. (b) A multimodal training pipeline. The UNet model is replicated for distributed data-parallel training.

transforms used are often embarrassingly parallel, e.g., randomly cropping one image for training. There have been numerous frameworks built to address this exact problem of scaling arbitrary distributed dataflows [1, 4, 7, 8, 17, 21, 27, 43]. Unfortunately, none of these are able to fully address the problem of efficient scaling of *heterogeneous* dataflows that use a mix of resources, e.g., GPUs and CPUs.

Resource heterogeneity requires pipelining execution across different operators to maximize overall utilization. For example, maximizing GPU utilization requires pipelining GPU compute with any CPU and I/O operations needed for data preprocessing, postprocessing, and loading. This introduces two requirements. First, *the system must manage memory for intermediate data between operators that require different resources*. This is challenging because the system must maximize overall throughput while ensuring sufficient overall memory. If too little intermediate data is buffered, the GPU will idle, wasting valuable resources. On the other hand, if too much data is buffered, the system may run out of memory or incur expensive overheads from swapping intermediate data to disk. This is especially important in multimodal applications, which often produce large intermediate outputs, e.g., one video file produces a series of decoded frames.

Second, *achieving efficiency in a heterogeneous setting requires elasticity to keep the overall pipeline balanced*, as the optimal resource allocation per data record and operator may not be known until run time. For example, in video generation,

*Equal contribution.

longer videos will take longer to process, so simple schemes like round-robin assignment of videos to resources can result in poor utilization. Ideally, the system should also be able to dynamically reallocate each operator’s resources based on actual load. Similarly, in the distributed setting, the system should be able to add and remove physical resources to the cluster with minimal downtime, including in unexpected cases such as node failures.

While there have been numerous frameworks built to scale traditional CPU-based data analytics, none achieve both of these requirements. Typically, they fall into one of two categories: *batch* or *streaming* systems. Batch systems [4, 8, 17, 43] divide the dataset into *partitions*, i.e. batches of data records (Figure 2a). Partitions can be processed by any executor, enabling elasticity and fine-grained recovery. However, batch systems process operators one at a time, which prevents pipelining and adds high memory overhead (Figure 3a). Streaming systems [1, 7, 21, 27] make the opposite tradeoff: they allow executors to buffer and send data directly to each other in dynamically sized batches (Figure 2b). This results in better utilization for heterogeneous resources and lower memory usage (Figure 3b). However, each operator and data range is bound to a specific set of resources, making it difficult to dynamically load-balance inputs, adjust resource allocations per operator, and scale the cluster.

We present Ray Data, a *streaming batch* system for heterogeneous workloads spanning batch inference and ML training. The key idea is to use *partitions* as the unit of execution to achieve elasticity, but to allow partitions to be dynamically created and streamed between heterogeneous operators for memory-efficient pipelining (Figure 2c). In Ray Data, a *partition* is a dynamically sized batch of records. Each partition is consumed by one or more *tasks*, each of which executes one (possibly fused) operator and dynamically produces one or more output partitions. *Tasks are dynamically assigned to resources* at run time, enabling elasticity as in batch systems while supporting pipelined execution across heterogeneous resources as in streaming systems (Figure 3c).

The key challenges stem from reconciliation of batch and streaming execution. First, batch systems also use partitions for resource elasticity but the partitions are typically fixed *before* run time. This is so that the system can correctly recover the partition in case of failure. However, because partition size determines memory footprint, this can lead to unpredictable memory usage at run time. Ray Data must therefore *size each partition based on real-time memory usage*. Second, when multiple operators require the same physical resource, avoiding stalls and data spills requires *joint control of memory allocation and compute resources*.

To address these challenges, Ray Data uses a centralized scheduler that dynamically partitions the dataset and assigns tasks to consume partitions. Executors can further dynamically partition their outputs based on actual memory usage to enforce cluster memory limits. The Ray Data scheduler uses

an online and memory-aware task scheduling policy, enabling joint control over cluster memory and compute resources at partition granularity. To maintain scalability, Ray Data builds on Ray [26] to decouple the control and data planes: the Ray Data scheduler issues partition control decisions but the partition data never flows through it.

We evaluate Ray Data on workloads spanning diverse resource requirements (CPUs, GPUs), storage (local, cloud), and modalities (text, image, video). Ray Data outperforms traditional batch and stream processing systems such as Spark and Flink by up to 12×. Ray Data matches the throughput of single-node data loaders specialized to ML training such as tf.data and PyTorch DataLoader while additionally leveraging disaggregated and heterogeneous preprocessing clusters. On a Stable Diffusion training benchmark, Ray Data improves training time by 31% by leveraging a pool of 704 CPUs and 72 heterogeneous GPUs. In summary, we contribute:

- The streaming batch model for memory-efficient and resource-elastic execution of heterogeneous distributed dataflows.
- An online scheduling policy for heterogeneous data processing that maximizes total compute utilization while enforcing total memory limits.
- Ray Data, an efficient, scalable, and fault-tolerant streaming batch system for heterogeneous ML applications.

2 Background

We overview key aspects and limitations of the batch and stream processing models (Table 1), including ML data loaders, by analyzing how effectively each system can:

- Maximize utilization of heterogeneous compute.
- Manage memory for intermediate data.
- Minimize overheads for cluster failures and re-scaling.

2.1 Applications

We target throughput for ML training and inference pipelines that require data pre- and post-processing using CPUs, GPUs, or both. Similar to current ML data loaders [28, 33], we primarily target map-style per-row transforms. We support operations that require all-to-all shuffle exchanges, such as sort and group-by, through techniques described in [24].

Figure 1a shows a typical batch inference pipeline, which uses CPUs to load a dataset from cloud storage, GPUs to produce predictions, then CPUs to upload the results. Figure 1b shows a typical multimodal distributed training pipeline, in this case for Stable Diffusion [35]. The pipeline uses CPUs to load image-text pairs, GPUs to run inference on frozen Encoder models, and GPUs to train a UNet model. Note that GPU operators can also benefit from heterogeneity and disaggregation: placing the Encoders on cheaper GPUs can reduce cost by allowing UNet more GPU memory (Section 5.2.2).

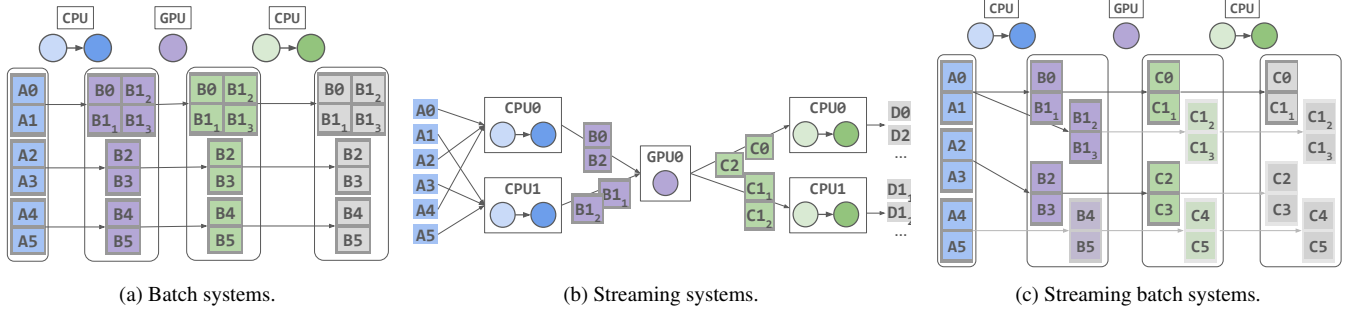


Figure 2: Execution plans for video generation (Figure 1a). A0, A1, etc. are data records. Consecutive operators that require the same resources are fused. A1 is a large video that decodes to 3 video segments, B1₁, B1₂, B1₃. (a) Before execution, batch systems divide the dataset into evenly sized partitions, e.g., the box with A0 and A1. At run time, partitions are assigned resources dynamically. (b) Before execution, streaming systems assign each executor resources and a range partition for an operator (e.g., even keys for CPU0). At run time, executors stream records in dynamically sized batches. (c) Before execution, streaming batch systems divide the *initial* dataset into partitions. At run time, partitions can be dynamically split and dynamically assigned resources. Lighter partitions indicate ones that have not yet been materialized.

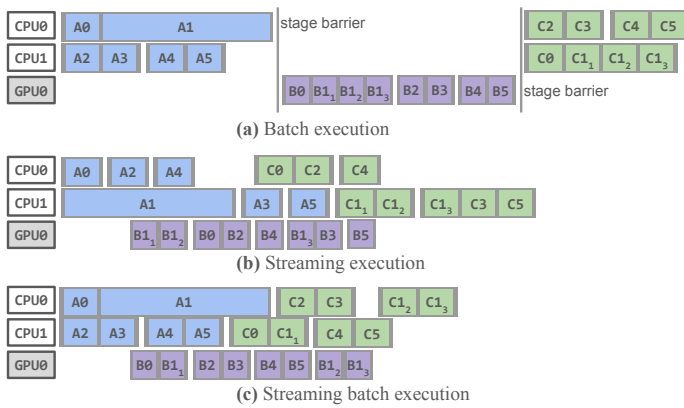


Figure 3: Execution timelines for Figure 2. (a) Batch systems dynamically assign partitions to resources but execute one stage at a time, materializing all intermediate partitions. (b) Streaming systems pipeline records between executors in dynamically sized batches but statically assign resources and records to executors, which can reduce utilization. (c) Streaming batch systems dynamically size partitions and dynamically assign partitions to resources for efficient pipelining and load-balancing.

2.2 Batch Processing Model

Batch processing systems use stateless tasks to allow a task to run and therefore recover on any executor. Examples include MapReduce [8], Apache Hadoop [4], Apache Spark [43], Spark Streaming [44], and Apache Flink in `BATCH` execution mode [7]. Before execution, the system transforms the logical DAG (Figure 1a) into a DAG of tasks and data partitions (Figure 2a). Tasks are stateless and materialize their input and output partition(s). This is key to lineage-based recovery, which avoids logging data by recording only the DAG and re-executing tasks to recover lost partitions. Elastic scaling is supported by simply adding or removing executors.

However, to make this recovery method practical, the system imposes two significant restrictions on execution. First, each stage must fully execute *before* executing the next

stage (Figure 3a). This simplifies scheduling and recovery, as a (re)scheduled task never idles waiting for its inputs, but prevents pipelining and requires materializing all outputs between stages. The consequences are not as severe in homogeneous applications because consecutive map operators that require the same resources can be fused into one stage (Figure 2a). In the heterogeneous setting, fusion of operators requiring different resources couples their parallelism, easily leading to under-utilization in heterogeneous clusters.

Second, the data partitioning must be determined *before* execution so it can be recorded in the lineage. This prevents the system from using run-time information such as the in-memory size of intermediate data rows when deciding the partitioning. Thus, even with pipelined stage execution, batch systems can still experience high memory pressure from single intermediate partitions that are too large. For example, Figure 2a shows a video generation case where the A1 video is significantly longer. Under the static partition plan, B0, B1₁, B1₂, B1₃ would remain in the same partition, which would now be twice as large as the others.

2.3 Stream Processing Model

Stream processing architectures optimize for low latency by using stateful executors that exchange records directly without involving a centralized scheduler. Examples include Naiad [27], Apache Flink [7], Spark Continuous Processing [39], MillWheel [1], and Apache Kafka [21]. Before execution, the system assigns resources to each executor, and then shards each logical operator across the executors. For example, in Figure 2b CPU0 is assigned the even indices for all CPU operators. Executors execute asynchronously: each can buffer records and decide when to send a batch to a downstream operator. If the downstream executor is overloaded, backpressure is applied to limit overall memory usage. This enables memory-efficient pipelining across heterogeneous operators.

However, this is achieved by coupling each executor to a set

of resources, operator(s), and data range(s), which prevents dynamic load balancing. Thus, cluster reconfiguration requires expensive protocols to maintain distributed state consistency. Some systems use *global checkpointing* [7, 27], which minimizes run-time overheads. However, *any* failure or reconfiguration event triggers a global rollback to the last checkpoint [7, 11]. Other systems use *logging* [1, 21], which enables fast recovery and reconfiguration by durably logging intermediate data. However, this adds high run-time overheads [27] that are unacceptable for ML pipelines, where most computations are idempotent and thus do not need durability.

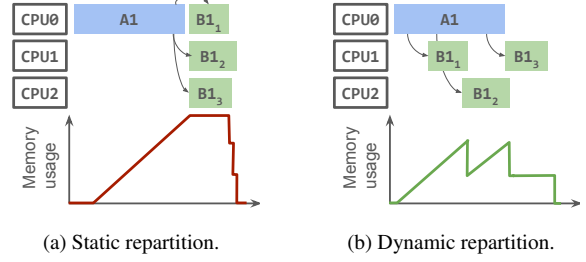
ML data loaders. ML data loaders such as `tf.data` [28] and PyTorch `DataLoader` [33] use CPUs to load data onto a local GPU. They can be viewed as single-node stream processing systems: they launch a fixed pool of worker threads or processes that continuously load, preprocess, and feed data to a GPU consumer. ML data loaders do not typically support distributed execution, which prevents load-balancing across nodes and the use of heterogeneous node types. Also, GPUs are assumed to be sinks, which precludes use cases such as batch inference that require CPU-based post-processing in addition to preprocessing.

3 Overview: The Streaming Batch Model

Streaming batch execution (Figures 2c and 3c) presents two challenges: (1) supporting dynamically sized partitions, and (2) dynamically assigning cluster resources to partitions.

Challenge 1: Dynamic partitioning. The throughput and memory footprint of a batch system is sensitive to the partition size. Our goal is to achieve memory-efficient pipelining without requiring users to tune a static partition plan. In particular, we want to allow the user to set only a target partition size in bytes, and the system should automatically partition intermediate data records at run time according to their actual memory usage. This is challenging because then the number of partitions is not known until run time. Meanwhile, batch systems typically require logging the partition plan *before* execution to enable lineage-based recovery.

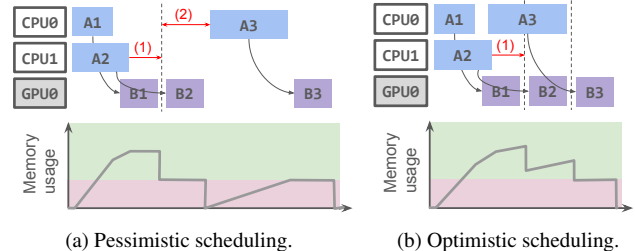
To address this, we propose dynamic partitioning (§ 4.2.1). The Ray Data scheduler decides the initial dataset partitioning (dataset A in Figure 2c) and maintains a global view of the current status of each partition. The scheduler submits tasks to process materialized partitions, and each task produces a stream of output partitions. Each executor locally decides how to partition its outputs based on the target partition size and real-time memory consumption. For example, in Figure 4b, the task processing A1 accumulates a buffer of output records. When the buffer reaches the target partition size, it flushes the buffer into the B1₁ partition. The task repeats this until it has outputted all records. This reduces peak memory usage by allowing another task to process and release B1₁ while A1 is executing, also seen in Figure 3c.



(a) Static repartition.

(b) Dynamic repartition.

Figure 4: Arrows represent data dependencies. (a) Batch systems allow repartitioning, but it must be specified by the user before execution. Execution across operators cannot be pipelined. (b) Streaming batch systems dynamically and automatically repartition outputs to reduce peak memory usage. This also allows the next operator to start in parallel with A1.



(a) Pessimistic scheduling.

(b) Optimistic scheduling.

Figure 5: Scheduling under memory pressure. Green represents CPU executors' local memory capacity (1 partition per CPU, 2 total). Pink represents the system's shared memory capacity for intermediate data (1 partition total). Arrows represent data dependencies. (1) indicates a period where executors must stall and buffer outputs locally until there is sufficient space in shared memory. (a) further stalls CPU0 during (2) until there is enough shared memory to schedule A3, while (b) schedules A3 as soon as possible.

To reduce load on the scheduler, we use Ray so that executors only need to return *references* to their output partitions back to the scheduler, not the data [41]. However, Ray requires tasks to return all outputs at once, and lineage-based recovery requires the number of outputs to be known ahead of time. We extend Ray's task scheduling and lineage subsystems to allow a task to stream its returned references (§ 4.2.2).

Challenge 2: Dynamic resource assignment. The centralized scheduler maintains a global view of the current partition plan (Figure 2c) and the available resources, allowing it to quickly reallocate resources to different operators at partition boundaries and implement cluster-level scheduling policies such as leveraging data locality to reduce data movement for distributed data-parallel training. However, efficient resource allocation for a heterogeneous pipeline is challenging and requires joint control with memory allocation.

For example, consider Figure 5a. Each CPU executor has local memory capacity (green) for 1 partition, and the system has shared memory capacity (pink) for 1 partition. In phase (1), A2 stalls and buffers its outputs locally until B1 completes. A conservative scheduler also waits for phase (2)

	Batch [4, 8, 17, 43]	Stream [1, 7, 21, 27]	PyTorch DL [33]	tf.data [28]	Streaming batch (Ray Data)
Dynamic partitioning	✗	✓	✗	✓	✓
Dynamic resource assignment	✓	✗	✗	✓ (local only)	✓
Fault tolerance method	Lineage	Logging/Checkpointing	None	Checkpointing	Lineage
Min. rollback granularity	Partition	Record/Epoch	Job	Epoch	Partition
Heterogeneous node types	✓	✓	✗	✗	✓

Table 1: Systems for heterogeneous data processing. *Dynamic partitioning*: the system decides how to batch records between operators. *Dynamic resource assignment*: the system dynamically assigns cluster resources to operators. *Rollback granularity*: the amount that needs to be re-executed upon failure or cluster reconfiguration. Streaming systems use logging for record-level rollback [1, 21] or global checkpointing for epoch-level rollback [7, 27]. Some ML data loaders support dynamic partitioning and resource assignment [28], but only within a node.

Method	Description
read	Read items from files.
map	Transform each item.
map_batches	Transform a batch of items. Useful for controlling GPU batch size.
flat_map	Transform each item and flatten the results.
filter	Return items that match a predicate.
limit	Truncate to the first N items.
write	Write items to files.
iter	Return an iterator of items.
iter_split	Split into N iterators.
cache	Materialize all items and cache in memory.

Table 2: A subset of the Ray Data Dataset API. The bottom four are consumption APIs that trigger execution, while the others are lazy.

before scheduling A3, to avoid stalling CPU0. Meanwhile, Figure 5b reduces overall run time by scheduling A3 optimistically so that it finishes simultaneously with B2. Applying such an optimization successfully would ideally require knowing A3’s run time and memory footprint.

Section 4.3 introduces our adaptive scheduler, which provides both policies in Figure 5. We use a conservative back-pressure mechanism similar to stream processing systems to implement Figure 5a. For Figure 5b, we use profile-guided optimization to estimate future memory availability, enabling robust optimistic scheduling. Because we use a centralized scheduler, both policies are simple to specify.

3.1 The Dataset API

A Dataset represents an application pipeline. Datasets are lazily created, by reading files or applying transforms to an existing Dataset (Table 2). A Dataset is materialized through a write to storage, by iterating over the items in memory, or via cache.

A key part of the API is the ability to express *resource requirements*. Resource requirements are a map from resource name to float value and may be passed as an option to each transform. By default, each transform requires 1 CPU. Resource names can be CPU, GPU, or a custom resource label.

The map transforms take a stateless user-defined function (UDF) as an argument. For operations that require significant

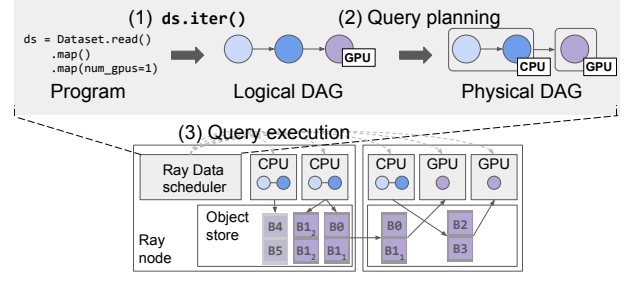


Figure 6: Ray Data architecture overview. Ray Data executes as a Ray library. The Ray Data scheduler maintains the partition metadata (Figure 2c) and dispatches tasks to Ray workers (dashed arrows).

initialization time, such as a model loaded into GPU memory, we also support UDFs with read-only state. Like other lineage-based systems, we assume that UDFs are pure.

3.2 Executing a Ray Data Program

After creating a Dataset, the user triggers execution by calling one of the consumption APIs, as seen in (1) in Figure 6. The Dataset is represented as a DAG of logical operators (Figure 1). The system’s query planner then compiles this logical DAG into a DAG of physical operators ((2) in Figure 6). The query planner applies operator fusion and decides the number of partitions to use for the first operator (§ 4.1).

Ray Data uses Ray as a task backend, storing intermediate data partitions in Ray’s distributed object store. During execution, the Ray Data scheduler maintains a global view of the current partition metadata (Figure 2c), including a reference to the remote data. The scheduler then dispatches each physical operator as a series of Ray tasks ((3) in Figure 6). Stateless UDF tasks are scheduled directly by Ray and can run on any Ray worker. For each stateful UDF, Ray Data creates a pool of Ray “actors”: stateful workers that acquire resources for their lifetime. If multiple stateful UDFs require the same resource, multiplexing is possible by sharing an actor pool between UDFs. Note that while actors hold read-only application state such as a GPU model, they do not store any system state, so any stateful UDF task can execute on any actor in the pool. This enables simple load balancing across

workers. Furthermore, reallocating an operator’s resources and scaling the cluster up or down simply requires updating the Ray Data scheduler’s map of available resources.

The Ray Data scheduler runs a continuous loop alternating between waiting for a dispatched task to materialize an output partition and release its resources, and choosing a new task to run on any available resources. In principle, one could instead rely entirely on Ray’s scheduler by submitting the entire task graph in [Figure 2a](#) upfront. However, this would prevent dynamic partitioning and naive application of Ray’s scheduler results in poor performance ([Section 5.3.3](#)), as Ray cannot easily implement the application-aware policies that we present in [Section 4.3](#).

4 System Design

4.1 Query Planning

The query planner transforms a logical DAG ([Figure 1](#)) into a physical DAG ([Figure 2a](#)), then applies optimizations such as operator fusion and the initial partitioning for `read`. We choose enough partitions to use all available execution slots (usually CPUs), but not so many that each partition is tiny, which can increase system overheads. If the estimated output size is known for a particular file type, then we also aim to produce partitions that are 1–128 MB in size ([Section 5.3.2](#)). Note that the system is robust to the initial number of partitions because we also dynamically repartition at run time.

Dataset consumption APIs ([Table 2](#)) are also incorporated into the physical DAG. The `Dataset.write` call is implemented with `map`. The `iter` API returns a stream of output records. This is implemented by fetching and buffering materialized output partitions. The `iter_split` call shards the outputs into N streams, each of which can be passed to a different reader process. This is useful for cases such as distributed data-parallel training where the dataset is sharded among N trainers. To implement `iter_split`, the query planner uses an additional Ray actor to coordinate dynamic assignment of materialized output partitions to readers.

4.2 Query Execution

During execution, the Ray Data scheduler maintains a global view of materialized partitions ([Figure 2c](#)), executing tasks and available resources. For each partition, the Ray Data scheduler maintains the following metadata: number of rows, size in bytes, and node location (used for data locality). For each operator, the scheduler maintains a queue of input partitions, stored as Ray references. It then repeatedly executes this loop:

- Wait for an executing task to materialize an output partition. Push the partition reference onto the downstream operator’s input queue. Tasks may produce multiple output partitions; if this was the last, free the task’s resources.

- While there are free resources and queued input partitions, select a physical operator to run using the policy described in [Section 4.3](#). Launch a new task for that operator. Mark the task’s required resources used.

To launch a new task, the scheduler passes a closure of the physical operator to execute and references to the task’s input partition(s). Ray ensures that all references are replaced by the physical data on the task executor. Typically, the scheduler will delete a reference as soon as its downstream task is submitted, signaling to Ray that the data can be garbage-collected after task execution. To implement `Dataset.cache()`, the scheduler simply keeps a reference to all output partitions of the corresponding operator.

4.2.1 Dynamic repartitioning

The query planner’s initial estimate of the number of partitions to use may not be optimal. Ray Data uses dynamic repartitioning to handle such cases. To support this, we extend Ray with *generator tasks*, enabling remote tasks to produce a dynamic number of outputs, and to pipeline execution with the task’s caller (the Ray Data scheduler). Whenever the task yields a new output partition, it notifies the Ray Data scheduler via RPC. Upon receipt, the scheduler reruns the scheduling loop and can launch a downstream task. Meanwhile, the upstream task continues producing its next output.

Ray Data executors take a target partition size from the scheduler and determine locally how to partition task outputs. A Ray Data task is an iterator that applies the given transform over its input partition(s). The executor yields from this iterator until the accumulated buffer exceeds the maximum target partition size (128 MB by default). Then, the Ray Data task flushes its buffer as a partition in Ray’s object store. For example, for a video decoding transform, Ray Data could assign one video per task, and each task would yield a stream of video frames. The Ray Data executor would then dynamically batch the frames into a stream of output partitions. Once the task finishes, all corresponding system state is removed from the executor.

Operators that produce much less data than they consume can produce too-small partitions. To handle this, the Ray Data scheduler coalesces partitions by passing multiple partitions from the upstream operator to a single task, up to the maximum target partition size.

For ML workloads, users often want control over GPU batch size. Thus, we expose a `map_batches` API that accepts a batch transform function and a target batch size. Ray Data tasks ensure the batch size by iterating over slices of the input partition(s). The Ray Data scheduler also coalesces too-small partitions to the desired batch size.

4.2.2 Failure recovery

Ray provides automatic recovery for objects (intermediate partitions) as long as (1) the driver is alive, (2) the tasks that created them are deterministic and side effect-free [41], and (3) the task arguments and outputs are immutable. For generator tasks, (3) is no longer true, because we do not know at submission time how many outputs the task will produce. However, we note that if (2) is true, then dynamic repartitioning can be made deterministic. In particular, given a target partition size and a pure transform, we ensure that a Ray Data task will produce the same stream of output partitions if executed on the same input partition(s).

To support failure recovery for generator tasks, we modify Ray’s recovery subsystem to handle tasks with an unknown number of outputs. On the first successful execution of a generator task, the task’s caller records the number of outputs that the task produces. If any of the task’s outputs are lost, we recover by re-executing the entire task. If the task produces a different number of outputs, we throw an error.

Similar to other batch and stream processing systems [7, 28, 32, 43], if the centralized scheduler dies, Ray garbage-collects the job and so Ray Data must re-execute from the beginning. Rollback can be reduced via checkpointing.

4.3 Scheduler Policy

The scheduler policy takes as input:

- The physical DAG of operators (Figure 6), each annotated with a resource requirement, e.g., {GPU:1}.
- Cluster resources: for each node, the number of CPU, GPU, or custom resource slots, and the memory capacity of the shared memory pool that stores partitions.

The scheduler policy decides the current mapping between cluster resources and operator tasks/partitions. Each time a task completes, the policy can allocate the freed resources to a new operator task. The policy can also choose to allow more than one outstanding task per cluster resource. This is beneficial for cases such as large language model (LLM) inference, which batches continuously across sequences for better throughput [42]. With multiple tasks in flight to an LLM replica, batching can be applied to sequences *across* partitions in addition to *within* a partition (Section 5.1.1).

The scheduler enforces the shared memory capacity as a hard limit, using either policy in Figure 5. We implement the pessimistic policy (Figure 5a) by prioritizing operators with shorter output queues and stalling in-progress tasks when the global memory limit has been reached. This is similar to the backpressure mechanism used in streaming systems. Next, we describe the optimistic policy that minimizes stalling based on run-time profiling.

Algorithm 1 Adaptive Scheduler

```

1: Initialize  $budget \leftarrow totalMemoryCapacity$ 
2: while not all operators are done do
3:   Update resource utilization and run-time estimates
4:   Update budget                                 $\triangleright$  Algorithm 2
5:   if  $budget \geq outputPartitionSize(source)$  then
6:     Launch task of  $source$ 
7:      $budget \leftarrow budget - outputPartitionSize(source)$ 
8:   end if
9:    $Q \leftarrow \emptyset$                            $\triangleright$  Set of qualified operators
10:  for each operator  $op$  in DAG do
11:    if  $hasInputData(op)$  and
12:       $hasAvailableResources(op)$  and
13:       $hasOutputBufferSpace(op)$  then
14:         $Q \leftarrow Q \cup \{op\}$ 
15:    end if
16:  end for
17:  if  $Q \neq \emptyset$  then
18:     $selected \leftarrow \arg \min_{op \in Q} bufferedOutputsSize(op)$ 
19:    Launch task of  $selected$ 
20:  end if
21: end while

```

4.3.1 Optimistic policy

The optimistic policy (Figure 5b) aims to minimize stalling and therefore job completion time by estimating when memory will become available in the *future*. To achieve this, the scheduler estimates and then equalizes the processing rates of each operator (in bytes per second). Intuitively, if processing rates are not equal, slower operators will accumulate pending inputs, eventually exhausting memory. The optimistic policy estimates operator processing rates online using run-time statistics: task durations and ratio of input:output size. The policy controls operator processing rates by deciding how many tasks to run in parallel for that operator.

Algorithm 1 describes the scheduling loop for the optimistic policy. Like the pessimistic policy, the optimistic policy prioritizes the operator with the least amount of buffered outputs. However, when memory is constrained, the policy (without lines 4–8) will result in resource under-utilization, as seen in Figure 5a. The ideal solution is to keep the pipeline full and start *source* tasks, i.e. tasks for the first operator, as early as possible, as in Figure 5b. To achieve this, lines 4–8 add a higher-priority optimistic policy for scheduling source tasks, described next.

The input rate, i.e. the rate at which source tasks are scheduled, must approximate the pipeline’s overall throughput. We use a dynamic *memory budget* algorithm to regulate the rate at which source tasks are launched. Intuitively, the budget is an optimistic estimate of the memory available for new data partitions to enter the system. When a source task is launched, we deduct its estimated output size from the budget. At every second, the budget is replenished using Algorithm 2, which

Algorithm 2 Memory Budget Update (runs every second)

```
1:  $P \leftarrow 0$             $\triangleright$  Total processing time per partition
2:  $\alpha_0 \leftarrow 1$          $\triangleright \alpha_i := \text{Input:Output size ratio for } op_i$ 
3: for  $i \leftarrow 1$  to  $numOps$  do
4:    $E_i \leftarrow \text{availableExecutionSlots}(op_i)$ 
5:    $T_i \leftarrow \text{estimatedTaskDuration}(op_i)$ 
6:   if  $op_i$  is not source then
7:      $I_i \leftarrow \text{estimatedInputSize}(op_i)$ 
8:      $O_i \leftarrow \text{estimatedOutputSize}(op_i)$ 
9:      $\alpha_i \leftarrow \alpha_{i-1} \cdot O_i / I_i$ 
10:    end if
11:     $P_i \leftarrow (T_i / E_i) \cdot \alpha_{i-1}$ 
12:     $P \leftarrow P + P_i$ 
13: end for
14:  $\text{budget} \leftarrow \text{budget} + \text{outputPartitionSize}(\text{source}) / P$ 
```

estimates the rate at which data leaves the pipeline. For DAGs with multiple sources, we launch each source operator at a rate proportionate to its output size.

We will walk through the algorithm using the following example: load (CPU) \rightarrow transform (CPU) \rightarrow inference (GPU) pipeline, running on a cluster with 8 CPUs and 4 GPUs.

- Consider the first non-source operator: transform. Suppose the current number of available execution slots to run the task is $E_1 = 6$ (out of 8 CPU slots). Assume the average task duration is $T_1 = 12$ seconds. Then the processing time of this stage is $P_1 = T_1 / E_1 \cdot \alpha_0 = 12 / 6 \times 1 = 2$, where α_0 , the output multiplier, is initialized to 1. In other words, transform takes 2s to process a source partition on average.
- Assume the transform’s average output is double the size of its input, i.e. $\alpha_1 = 2$. Now consider inference. Assume the number of available execution slots is $E_2 = 4$ (GPU), and the average task duration is $T_2 = 2$ seconds. Then $P_2 = T_2 / E_2 \cdot \alpha_1 = 2 / 4 \times 2 = 1$, i.e. the inference operator takes 1 second per source partition.
- Adding them up, $P = 2 + 1 = 3$ seconds per source partition. In other words, every ~ 3 s, the budget will be replenished to allow for one more source task to run.

If the run-time estimates of each operator’s processing rates are perfectly accurate, i.e. if there is no variance in the processing rates, it can be shown that the schedule produced is optimal. However, when there is variance in processing times or output sizes, the budget algorithm could overestimate the overall processing rate. Nevertheless, the algorithm is stable because it creates a negative feedback loop. If it overestimates the pipeline processing rate, more source tasks might launch and temporarily cause backpressure, or objects in the buffer to spill to disk. However, because these tasks occupy execution slots, they will reduce the parallelism of downstream operators and lower the replenishment rate of the budget, which in turn limits the source task launch rate.

4.4 Implementation

We implement Ray Data on top of Ray because Ray exposes a low-level execution model based on dynamic task execution, with powerful features such as automatic data movement, lineage-based recovery [41], and disk spilling [24]. This makes it convenient to build centralized schedulers like Ray Data while leveraging Ray as a decentralized dataplane. However, Ray also treats the task logic, inputs, and outputs as black boxes. Thus, it is difficult to directly extend Ray with data processing-specific features such as dataset partitioning and pipeline-aware task scheduling. Instead, we implement Ray Data as a Ray library, which allows us to build such features with minimal changes to the Ray core. Ray Data is an industrial system and is written in ~ 51 k Python LoC, with about 1k, 1k, and 2k LoC for the query planner, scheduler, and map executor logic, respectively.

5 Evaluation

We evaluate heterogeneous workloads in batch (offline) inference and training, including retrieval-augmented LLM generation (RAG) and multimodal models. We use benchmarks taken from the MLPerf suite [25, 34], and supplement with additional LLM, image, and video benchmarks. We study:

- § 5.1: How does Ray Data compare to batch or stream processing systems when running heterogeneous ML workloads, in terms of throughput and elasticity?
- § 5.2: How can distributed and heterogeneous execution reduce cost compared to single-node training data loaders?
- § 5.3: How well can all systems adapt to memory pressure from intermediate data in heterogeneous settings?

We compare the following systems:

- Batch processing (Section 2.2): Apache Spark 3.5.1.
- Stream processing (Section 2.3): Apache Flink 1.19.0.
- Single-node ML data loaders (Section 2.3): tf.data [28] and PyTorch DataLoader (PyTorch DL) [33]. tf.data can reconfigure the number of threads per operator.
- Streaming batch: Ray Data (implemented over Ray 2.40.0). We also modify Ray Data to emulate batch processing (Ray Data-staged) and stream processing (Ray Data-static), for apples-to-apples comparison of the execution models. Ray Data-staged materializes each stage before starting the next, while Ray Data-static sets a static parallelism per operator and replaces the dynamic scheduler (§ 4.3) with round-robin partition assignment.

For training workloads, we compare only against tf.data and PyTorch DataLoader because these systems were custom-built for data preprocessing for training. We use Spark, Flink, and Ray Data variants as comparisons for batch inference.

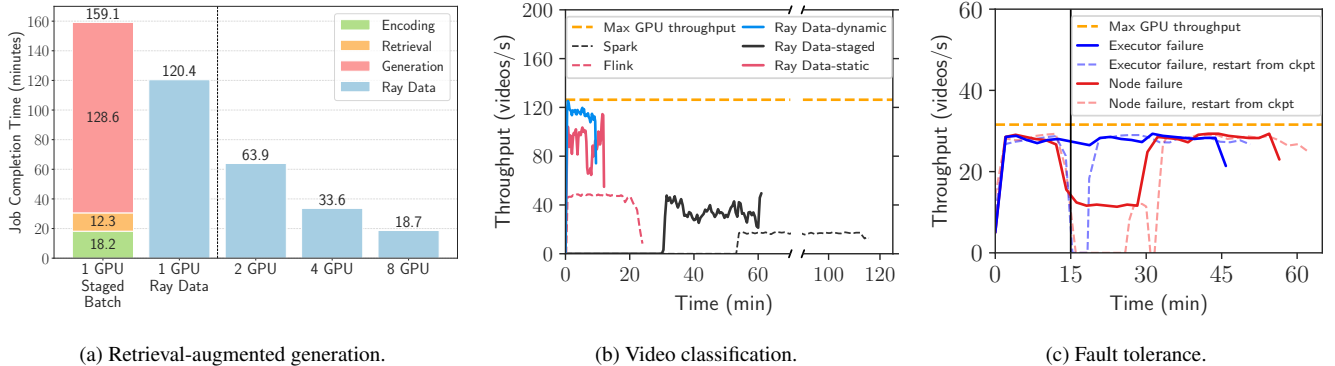


Figure 7: (a) RAG job completion time. “Staged Batch” runs stages sequentially in one process; its *Retrieval* run time is the optimal JCT if CPU is the bottleneck. (b) Video classification throughput comparison of batch (Spark and Ray Data-staged), streaming (Flink and Ray Data-static), and streaming batch (Ray Data-dynamic) systems. (c) Fault tolerance comparison for video classification on a heterogeneous cluster with 1 GPU node and 1 CPU-only node. Executor (blue) or node (red) failure is injected at $t=15\text{min}$. For node failure curves, the node is added back to the cluster at $t=30\text{min}$. The dashed line is a variant of Ray Data that emulates checkpoint-and-restore. This strategy leads to job downtime after every cluster change and longer completion time. Unmodified Ray Data (solid) smoothly handles executor failure and node failure and addition.

5.1 Inference: Ray Data vs. batch and stream processing

5.1.1 Retrieval-Augmented Generation (RAG)

RAG [23] improves LLM inference accuracy by retrieving relevant documents from a knowledge base to augment the original prompt. Our RAG pipeline consists of three stages: (1) *encode* (CPU): Encode the input prompt using a pre-trained encoder (Contriever [18]) to produce a dense embedding. (2) *retrieve* (CPU): Use a FAISS [10] vector index to retrieve the top- k most similar documents from the knowledge base (TriviaQA [19]). (3) *generate* (GPU): Serve the Llama-3-8B model [14] with vLLM [22] to generate the final output based on the input prompt and retrieved documents. We run the RAG pipeline on 1 node with 8 H200 GPUs and 256 CPUs.

Figure 7a shows the job completion time (JCT) for 100K prompts. We compare Ray Data to a single-process baseline “Staged Batch” that sequentially executes each stage. On 1 GPU, Ray Data achieves 1.32x speedup compared to the baseline. This is because Ray Data runs all stages concurrently and overlaps the CPU- and GPU-based stages, so its overall JCT is similar to that of the *generate* stage in “Staged Batch”.

We also scale Ray Data to multiple GPUs. On N GPUs, we use Ray Data to set the parallelism of *generate* to N , creating N vLLM replicas. As shown in Figure 7a, compared to 1 GPU, Ray Data is able to achieve 1.88x speedup for 2 GPUs, 3.58x speedup for 4 GPUs, and 6.44x speedup for 8 GPUs. Larger overhead is observed when scaling from 4 to 8 GPUs because the CPU-based stages become the bottleneck.

Takeaways: (1) Ray Data outperforms batch processing via asynchronous stage execution, and (2) Ray Data scales LLM inference via data parallelism while saturating the resource bottleneck, either GPU or CPU.

5.1.2 Video Classification

We run the VideoMAE video classification model [38] on the test split of the Kinetics-700-2020 dataset (64,535 videos, 137.3 GB, Amazon S3), on 4 g5.2xlarge nodes (8 vCPUs, 1 NVIDIA A10G GPU each). The operators are: (1) *read*: download and read binary files from S3, (2) *preprocess*: decode a video into a series of frames, (3) *map_batches* (VideoMAE): classify video frames using a GPU-hosted model. Figure 7b shows throughput over time. We include Ray Data-staged and Ray Data-static to emulate batch and streaming systems, respectively.

Batch systems (Spark and Ray Data-staged) execute stages synchronously, so they do not produce results until $t=53\text{min}$ and $t=31\text{min}$ for Spark and Ray Data-staged, respectively. Also, the JCTs are $t=116\text{min}$ and $t=61\text{min}$ respectively because all intermediate stage results are materialized and must be spilled to disk to avoid OOM.

Streaming systems (Flink and Ray Data-static) pipeline across heterogeneous operators so they are able to produce results almost immediately. However, they are also sensitive to the static assignment of operator ranges to executors. Both use a round-robin approach to assign data to executors. Flink’s throughput is more stable than Ray Data-static’s until $t=20\text{min}$, likely due to finer-grained batching. However, Flink also has significant overheads from serializing and copying data between Java and Python. Thus, we also include Ray Data-static for fair comparison. Ray Data-static’s throughput is unstable due to lack of dynamic load balancing.

Ray Data-dynamic is our streaming batch system, which dynamically creates and schedules partitions. This is the same as Ray Data-static, except that we replace the round-robin approach for assigning partitions with the scheduling policy described in Section 4.3. This achieves 88.4% of the optimal

run time based on maximum GPU throughput, and $2.5\times$ and $1.25\times$ better than Flink and Ray Data-static, respectively.

Takeaways: (1) Streaming and streaming batch systems outperform batch systems through memory-efficient pipelining, (2) Ray Data’s dynamic resource assignment further improves throughput compared to the static assignment often used in streaming systems.

5.1.3 Fault tolerance in heterogeneous clusters

We use the same workload as in Section 5.1.2 to demonstrate Ray Data’s ability to scale using clusters with heterogeneous node types and to smoothly scale clusters up and down, including during failures. Figure 7c shows the throughput during failure recovery when processing 10% of the dataset using a cluster with 1 g5.xlarge node (4 vCPU, 1 GPU) and 1 m7i.2xlarge node (8 vCPU). For all systems, we inject a node or executor failure at $t=15\text{min}$. Executor failure kills one worker process. Node failure disconnects the CPU-only node and reconnects it at $t=30\text{min}$. We compare Ray Data (solid curves) against Ray Data modified to emulate the global checkpoint strategy used in many stream processing systems. The modified Ray Data (dashed curves) takes an empty checkpoint every 6min.

With checkpointing, both executor and node failures force a global rollback, causing downtime until the system recovers the lost work. Downtime under node failure is longer because the system has fewer resources while the CPU-only node is disconnected. Adding the CPU-only node back at $t=30\text{min}$ forces another global rollback. Meanwhile, Ray Data has no noticeable throughput drop under executor failure, and scales smoothly with cluster size during node removal and addition. **Takeaways:** Compared to streaming systems that use global checkpointing, Ray Data achieves similar run-time overhead. Meanwhile, Ray Data also smoothly handles CPU failures and cluster reconfiguration events.

5.2 Training: Ray Data vs. ML data loaders

5.2.1 ResNet Training

We run the ResNet-50 ImageNet training benchmark from MLPerf [25]. The data preprocessing pipeline loads images from local disk (local) or cloud storage (S3), decodes, and randomly crops and flips the images. We compare training throughput vs. tf.data on a g5.2xlarge VM. We do not measure PyTorch DL, as tf.data showed comparable or better results for the same benchmark [28].

Figure 8a shows training throughput over time. tf.data executes data preprocessing using a pool of worker threads running in each GPU trainer process. Thus, the job fate-shares with *any* preprocessing task that fails due to out-of-memory (OOM). When reading data from local disk, tf.data’s throughput is 19% lower than Ray Data’s because a lower batch size was required to prevent OOM failures. Meanwhile, Ray

Data is able to complete because GPU trainer failures are isolated from CPU worker failures, and CPU workers can be respawned in seconds, without impacting pipeline throughput (§ 5.1.3).

When reading data from S3, tf.data is 88% slower than the max GPU throughput because S3 loading is the bottleneck and the GPU’s local CPUs are insufficient. Meanwhile, Ray Data (S3) adds a CPU-only m7i.2xlarge node to scale out S3 loading independent of the GPU trainers. This achieves an overall training throughput of 93% of the maximum GPU throughput.

Takeaways: Compared to single-node ML data loaders, Ray Data offers: (1) failure isolation between heterogeneous resources, and (2) ability to leverage heterogeneous node types.

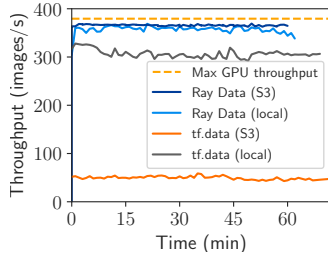
5.2.2 Pre-Training Stable Diffusion

Pre-training of large multimodal models is one of the most demanding heterogeneous workloads. We run the Stable Diffusion (SD) pre-training pipeline shown in Figure 1b and compare different execution modes. We execute 1 training epoch over a dataset of 2B images, on a cluster of $4\times$ p4de.4xlarge nodes, with 8 A100 GPUs each. This pipeline requires both CPUs and GPUs for data preprocessing: (1) `loadText/loadImage+clip` (CPU): Load and preprocess pairs of image and text, (2) `Encoder` (GPU): Use pre-trained encoder models for image and text to produce embeddings, and (3) `UNet.train()` (GPU): Train SD, using PyTorch fully-sharded data parallelism (FSDP) [46].

Figure 8b shows training throughput and total cost. PyTorch DL is a data loader custom-built for PyTorch that statically assigns work to a process pool. Its throughput is lowest because `Encoder` preprocessing competes with trainers for GPU memory. Ray Data-staged emulates batch processing by running data preprocessing as an offline job and storing precomputed embeddings in cloud storage. This is preferable if the same embeddings are used multiple times. Ray Data-staged achieves 19% higher throughput because `UNet` can use more GPU memory and therefore a larger batch size.

Ray Data runs all data preprocessing concurrently with training. This is preferable if using random transforms or for iterative development. Ray Data also disaggregates `Encoder` and `UNet`, placing `Encoder` onto cheaper A10G GPUs (g5.2xlarge). This results in 31% better throughput than PyTorch DL, because `UNet` has full GPU resources, and 15% better throughput than Ray Data-staged, because embeddings are kept in memory.

Takeaways: Compared to existing ML data loaders, Ray Data can: (1) be used for both batch and online data preprocessing, and (2) leverage clusters with heterogeneous GPUs.



(a)

	Resources	Images/s	Run time (hours)	Total cost
PyTorch DL (stream)	4 × p4de.24xlarge	2,811	111.3	\$18,192
Ray Data-staged (batch)	4 × p4de.24xlarge	0, then 4,068	90.3 (-19%)	\$14,753 (-19%)
Ray Data (streaming batch)	4 × p4de.24xlarge 40 × g5.2xlarge	4,075	76.8 (-31%)	\$16,275 (-11%)

(b)

Figure 8: (a) Training ResNet-50, loading data from local disk vs. cloud storage (S3). All experiments run on 1 g5.2xlarge node (1 NVIDIA A10G GPU, 8 vCPUs), except for Ray Data (S3), which uses an additional m7i.2xlarge (8 vCPUs) node to scale out S3 loading. (b) Run time and cost for one epoch of Stable Diffusion pre-training.

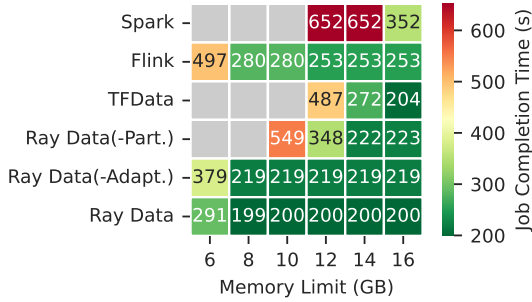


Figure 9: Run times for systems under different memory limits on a synthetic benchmark. Grey means the system is unable to finish due to OOM. Ray Data(-Part.) means Ray Data without dynamic repartition (Section 4.2.1). Ray Data(-Adapt.) means Ray Data without adaptive memory-aware scheduling (Section 4.3.1).

5.3 Microbenchmarks

5.3.1 Memory-aware pipelining

We evaluate how batch, streaming, and streaming batch systems schedule heterogeneous pipelines with and without memory pressure. The 3-stage pipeline is: (1) Load (CPU): 160 tasks, each producing 500 1 MB rows after 5s, (2) Transform (CPU): sleep for 0.5s per row, then return a new 1 MB row, (3) Inference (GPU): 0.5s per batch of 100 rows. We use 1 m6i.2xlarge node with 8 vCPUs, 4 simulated GPU slots, and 32 GB RAM. The theoretical best job completion time with unlimited memory is $(160 \times 5s + 800 \times 0.5s)/8 = 150s$.

Figure 9 shows job completion time vs. total memory limit. We limit memory through system-specific configurations, e.g., executor memory for Spark. We use POSIX `rlimit` to verify that each system respects its memory limit, and tune each system’s parallelism (e.g., executor count) if not.

Spark materializes all data between stages, achieving at best $2.35 \times$ optimal run time. At 12–14GB memory, Spark must use fewer executors resulting in $4.34 \times$ the optimal run time, and at lower memory limits, Spark OOMs. This is because Spark uses static partitioning, which is sensitive to memory pressure (§ 2.2).

Flink is less sensitive to the memory limit than Spark and achieves up to $1.68 \times$ optimal. This is because executors dy-

namically batch outputs and apply backpressure to avoid OOM (§ 2.3). Under lower memory limits, Flink must run fewer executors because each CPU slot is multiplexed among multiple physical operator threads. This results in up to $2 \times$ worse throughput.

tf.data offers an adaptive scheduler and memory budget, similar to Ray Data, albeit non-distributed. However, we found that the memory budget was not always enforced, requiring manual tuning of the thread count. tf.data achieves the same throughput as Ray Data at 16 GB memory limit, but OOMs at lower memory limits.

Ray Data achieves $1.3 \times$ the optimal run time at all memory limits except the lowest. We also conduct ablation studies. Ray Data(-Part.) disables Ray Data’s dynamic repartition (Section 4.2.1), resulting in too-large partitions similar to Spark. Ray Data(-Adapt.) uses Ray Data’s pessimistic policy instead of its optimistic policy (§ 4.3.1), resulting in 10–88% worse performance than Ray Data. Ray Data is also less sensitive than Flink to memory pressure because the system explicitly time-slices executors, instead of using multithreading.

Takeaways: For heterogeneous applications under memory pressure, batch processing systems are unstable. Ray Data is as stable as stream processing systems, due to its dynamic repartition, and it can further leverage run-time profiling.

5.3.2 Overhead of partitioning

Ray Data uses dynamic repartitioning with a centralized scheduler. Figure 10a evaluates Ray Data’s system overhead by measuring throughput vs. partition size on a 2-stage synthetic pipeline. We use 8192×1 MB input rows, and simulate 10 ms processing time per row per stage. The smallest partition sizes incur overhead from RPCs and bookkeeping, and the largest result in poor load-balancing. To strike a balance, Ray Data’s default target partition size is 128 MB.

5.3.3 Scalability

To evaluate the scalability of Ray Data, we run an empty workload which creates then consumes a large dataset on the cluster. We use 1 m8i.4xlarge (16 vCPU, 64GiB RAM) as the head node and up to 32 m8i.2xlarge (8 vCPU, 32GiB

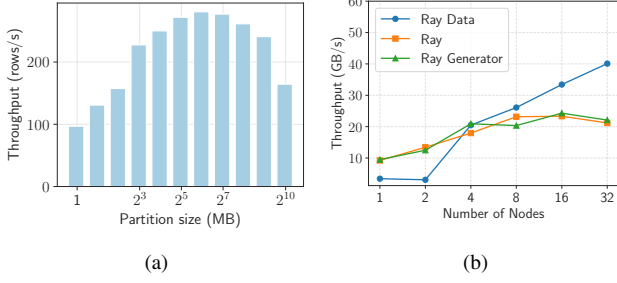


Figure 10: (a) Effect of partition sizes on throughput in Ray Data. (b) Scalability experiment showing throughput over number of nodes compared to using raw Ray tasks or generator tasks (Ray Generator).

RAM) worker nodes. The size of the dataset is proportional to the number of nodes in the cluster, with 5GB per node. We compare Ray Data against two baselines: Ray and Ray Generator. Ray Data uses the default partition size of 128MB. Ray spawns tasks that each return 128MB of data, then immediately passes each result to a consumer task. Ray Generator does the same, except that it uses the generator tasks described in Section 4.2.1.

Figure 10b shows the throughput versus the number of nodes in the cluster. Ray Generator achieves similar throughput as Ray; this validates that our extensions to Ray to support generator tasks (Section 4.2.1) add negligible overhead. Ray Data achieves worse throughput than Ray and Ray Generator on clusters with ≤ 2 nodes because of warmup time from its additional query planning step (Section 4.1). However, Ray Data scales linearly and delivers up to $1.8\times$ better throughput than Ray and Ray Generator on larger clusters. This is due to its application-aware scheduling policy (Section 4.3), which uses the high-level dataflow graph (Figure 1) to improve load balancing and avoid unnecessary spilling.

6 Related Work

Unifying batch and stream processing systems. Other systems that aim to unify the batch and stream models include Naiad [27], Flink’s batch execution mode [7], and Spark’s Discretized Streams (D-Streams) [44]. Naiad shows that the stream processing model is suitable for producing results both incrementally and in bulk, but it does not support dynamic resource assignment. Flink’s batch mode executes using synchronous stages, with the same limitations as other batch processing systems (Section 2.2).

Spark D-Streams and Drizzle [40] are batch systems that execute over infinite data streams. They partition the input stream into “microbatches”, each executed as a distinct job and typically one at a time. Internally, each microbatch job uses synchronous stage execution. If different microbatches were pipelined, it can be viewed as a form of the streaming batch model, but with three limitations: (1) the pipeline granularity is a microbatch job instead of a partition within

a microbatch, (2) each microbatch is treated as a separate job, so scheduling and data movement across microbatches is challenging, and (3) data partitioning is still static.

MillWheel [1] is a stream processing system that offers efficient reconfiguration and failover by combining decentralized physical logging with a centralized asynchronous load-balancer. It offers sophisticated APIs for real-time processing, including timers, watermarks, etc. In contrast, Ray Data targets offline processing, uses lineage-based recovery to avoid data logging, and the centralized scheduler dispatches *all* tasks for a global view and more control over resources.

Other efforts [2, 3] aim to unify streaming and batch execution but only at the API layer.

Scheduling for resource heterogeneity. The scheduling problem described in Section 4.3 is most similar to the generalized processor sharing [31] problem. Our solution is inspired by the weighted fair queueing algorithm [6, 9]. The differences are (1) the flows in network scheduling are independent of each other, whereas operators in a data pipeline have dependencies, (2) we consider multiple resource types, and (3) the packet processing time is usually fixed, whereas data operator processing times are unpredictable.

Recent scheduling works attempt to adapt fair queuing and autotuning to heterogeneous resource environments. Dominant resource fair queuing [13] addresses the problem of (2) but not (1) or (3). tf.data [28] introduces an autotuning algorithm that uses gradient descent to find the parallelism for each operator that reduces end-to-end latency.

Data loaders for ML training. Both PyTorch [32] and TensorFlow (tf.data [28]) provide map-style data loaders for ML training. tf.data automatically shards the dataset, while PyTorch DL requires the user to shard the dataset themselves. Both are single-node systems colocated with a GPU trainer and share similar limitations: they cannot leverage CPU-only nodes, load-balancing must be done by sharding before execution, and the training job fate-shares with the data loader.

tf.data service [5] improves upon these by enabling disaggregated CPU-based preprocessing for training. Ray Data provides a similar set of features and additionally provides exactly-once semantics (as opposed to at-most-once), GPU-based preprocessing, and batch inference support. Several recent works propose query optimizers for training preprocessing [15, 45]. These are complementary to Ray Data.

7 Discussion

Achieving native performance with a Python system is an important practical consideration for the modern ML ecosystem. One benefit of building Ray Data as a Ray library rather than as a monolithic system such as Spark or Flink is the ability to write Ray Data in pure Python. The Ray core is in C++, which avoids some of the overheads of exposing a Python frontend compared to systems built on non-native languages. Another

benefit is that it is easy to modify the Ray Data scheduler, as it is written at the library level.

Ray Data enables another key opportunity in future data processing systems: dynamic query planning. In this work, we present an online scheduler, but still make certain planning decisions statically, including the number of input partitions (Section 4.1), and the user specifies the initial cluster shape. In the future, we envision a fully autotuning and autoscaling system that can jointly configure the application and cluster.

Conclusion. With the rise of LLMs, even modalities such as text may now require expensive deduplication [29], retrieval (Section 5.1.1), GPU-based encoding, and joins with image or video data (Figure 1b). Also, as the parallelism strategies used in inference and training pipelines become more complex, future data processing systems must support more flexible APIs for sharding and reducing data copies.

We believe that ML systems will continue to grow in the complexity of their data processing needs, as evidenced by trends such as test-time training [12, 36], RAG [23], and multimodal models [30, 37]. To keep up with this demand, we must build more flexible, heterogeneity-aware, and scalable data processing systems.

References

[1] Tyler Akidau, Alex Balikov, Kaya Bekiroğlu, Slava Chernyak, Josh Haberman, Reuven Lax, Sam McVeety, Daniel Mills, Paul Nordstrom, and Sam Whittle. Mill-wheel: Fault-tolerant stream processing at internet scale. *Proceedings of the VLDB Endowment*, 6(11):1033–1044, 2013.

[2] Tyler Akidau, Robert Bradshaw, Craig Chambers, Slava Chernyak, Rafael J. Fernández-Moctezuma, Reuven Lax, Sam McVeety, Daniel Mills, Frances Perry, Eric Schmidt, and Sam Whittle. The dataflow model: a practical approach to balancing correctness, latency, and cost in massive-scale, unbounded, out-of-order data processing. *Proc. VLDB Endow.*, 8(12):1792–1803, aug 2015.

[3] Apache Software Foundation. Apache beam. <https://beam.apache.org>, May 2024.

[4] Apache Software Foundation. Apache hadoop. <https://hadoop.apache.org>, May 2024.

[5] Andrew Audibert, Yang Chen, Dan Graur, Ana Klimovic, Jiří Šimša, and Chandramohan A Thekkath. tf. data service: A case for disaggregating ml input data processing. In *Proceedings of the 2023 ACM Symposium on Cloud Computing*, pages 358–375, 2023.

[6] Jon C. R. Bennett and Hui Zhang. Wf2q: worst-case fair weighted fair queueing. In *Proceedings of the Fifteenth Annual Joint Conference of the IEEE Computer and Communications Societies Conference on The Conference on Computer Communications - Volume 1*, INFOCOM’96, page 120–128, USA, 1996. IEEE Computer Society.

[7] Paris Carbone, Asterios Katsifodimos, Stephan Ewen, Volker Markl, Seif Haridi, and Kostas Tzoumas. Apache flink: Stream and batch processing in a single engine. *The Bulletin of the Technical Committee on Data Engineering*, 38(4), 2015.

[8] Jeffrey Dean and Sanjay Ghemawat. Mapreduce: simplified data processing on large clusters. *Communications of the ACM*, 51(1):107–113, 2008.

[9] A. Demers, S. Keshav, and S. Shenker. Analysis and simulation of a fair queueing algorithm. In *Symposium Proceedings on Communications Architectures & Protocols, SIGCOMM ’89*, page 1–12, New York, NY, USA, 1989. Association for Computing Machinery.

[10] Matthijs Douze, Alexandr Guzhva, Chengqi Deng, Jeff Johnson, Gergely Szilvassy, Pierre-Emmanuel Mazaré, Maria Lomeli, Lucas Hosseini, and Hervé Jégou. The faiss library. 2024.

[11] E. N. (Mootaz) Elnozahy, Lorenzo Alvisi, Yi-Min Wang, and David B. Johnson. A survey of rollback-recovery protocols in message-passing systems. *ACM Comput. Surv.*, 34(3):375–408, September 2002.

[12] Yossi Gandelsman, Yu Sun, Xinlei Chen, and Alexei A Efros. Test-time training with masked autoencoders. In Alice H. Oh, Alekh Agarwal, Danielle Belgrave, and Kyunghyun Cho, editors, *Advances in Neural Information Processing Systems*, 2022.

[13] Ali Ghodsi, Vyas Sekar, Matei Zaharia, and Ion Stoica. Multi-resource fair queueing for packet processing. In *Proceedings of the ACM SIGCOMM 2012 conference on Applications, technologies, architectures, and protocols for computer communication*, pages 1–12, 2012.

[14] Aaron Grattafiori, Abhimanyu Dubey, Abhinav Jauhri, Abhinav Pandey, Abhishek Kadian, Ahmad Al-Dahle, Aiesha Letman, Akhil Mathur, Alan Schelten, Alex Vaughan, Amy Yang, Angela Fan, Anirudh Goyal, Anthony Hartshorn, Aobo Yang, Archi Mitra, Archie Srivankumar, Artem Korenev, Arthur Hinsvark, Arun Rao, Aston Zhang, Aurelien Rodriguez, Austen Gregerson, Ava Spataru, Baptiste Roziere, Bethany Biron, Binh Tang, Bobbie Chern, Charlotte Caucheteux, Chaya Nayak, Chloe Bi, Chris Marra, Chris McConnell, Christian Keller, Christophe Touret, Chunyang Wu, Corinne Wong, Cristian Canton Ferrer, Cyrus Nikolaidis, Damien Allonsius, Daniel Song, Danielle Pintz, Danny Livshits, Danny Wyatt, David Esiobu, Dhruv Choudhary,

Dhruv Mahajan, Diego Garcia-Olano, Diego Perino, Dieuwke Hupkes, Egor Lakomkin, Ehab AlBadawy, Elina Lobanova, Emily Dinan, Eric Michael Smith, Filip Radenovic, Francisco Guzmán, Frank Zhang, Gabriel Synnaeve, Gabrielle Lee, Georgia Lewis Anderson, Govind Thattai, Graeme Nail, Gregoire Mialon, Guan Pang, Guillem Cucurell, Hailey Nguyen, Hannah Korevaar, Hu Xu, Hugo Touvron, Iliyan Zarov, Imanol Arrieta Ibarra, Isabel Kloumann, Ishan Misra, Ivan Evtimov, Jack Zhang, Jade Copet, Jaewon Lee, Jan Geffert, Jana Vranes, Jason Park, Jay Mahadeokar, Jeet Shah, Jelmer van der Linde, Jennifer Billock, Jenny Hong, Jenya Lee, Jeremy Fu, Jianfeng Chi, Jianyu Huang, Jiawen Liu, Jie Wang, Jiecao Yu, Joanna Bitton, Joe Spisak, Jongsoo Park, Joseph Rocca, Joshua Johnstun, Joshua Saxe, Jun-teng Jia, Kalyan Vasuden Alwala, Karthik Prasad, Kartikeya Upasani, Kate Plawiak, Ke Li, Kenneth Heafield, Kevin Stone, Khalid El-Arini, Krithika Iyer, Kshitiz Malik, Kuenley Chiu, Kunal Bhalla, Kushal Lakhota, Lauren Rantala-Yeary, Laurens van der Maaten, Lawrence Chen, Liang Tan, Liz Jenkins, Louis Martin, Lovish Madaan, Lubo Malo, Lukas Blecher, Lukas Landzaat, Luke de Oliveira, Madeline Muzzi, Mahesh Pasupuleti, Mannat Singh, Manohar Paluri, Marcin Kardas, Maria Tsimpoukelli, Mathew Oldham, Mathieu Rita, Maya Pavlova, Melanie Kambadur, Mike Lewis, Min Si, Mitesh Kumar Singh, Mona Hassan, Naman Goyal, Narjes Torabi, Nikolay Bashlykov, Nikolay Bogoychev, Niladri Chatterji, Ning Zhang, Olivier Duchenne, Onur Çelebi, Patrick Alrassy, Pengchuan Zhang, Pengwei Li, Petar Vasic, Peter Weng, Prajjwal Bhargava, Pratik Dubal, Praveen Krishnan, Punit Singh Koura, Puxin Xu, Qing He, Qingxiao Dong, Ragavan Srinivasan, Raj Ganapathy, Ramon Calderer, Ricardo Silveira Cabral, Robert Stojnic, Roberta Raileanu, Rohan Maheswari, Rohit Girdhar, Rohit Patel, Romain Sauvestre, Ronnie Polidoro, Roshan Sumbaly, Ross Taylor, Ruan Silva, Rui Hou, Rui Wang, Saghar Hosseini, Sahana Chennabappa, Sanjay Singh, Sean Bell, Seohyun Sonia Kim, Sergey Edunov, Shaoliang Nie, Sharan Narang, Sharath Raparthy, Sheng Shen, Shengye Wan, Shruti Bhosale, Shun Zhang, Simon Vandenhende, Soumya Batra, Spencer Whitman, Sten Sootla, Stephane Collot, Suchin Gururangan, Sydney Borodinsky, Tamar Herman, Tara Fowler, Tarek Sheasha, Thomas Georgiou, Thomas Scialom, Tobias Speckbacher, Todor Mihaylov, Tong Xiao, Ujjwal Karn, Vedanuj Goswami, Vibhor Gupta, Vignesh Ramanathan, Viktor Kerkez, Vincent Gonguet, Virginie Do, Vish Vogeti, Vítor Albiero, Vladan Petrovic, Weiwei Chu, Wenhan Xiong, Wenyin Fu, Whitney Meers, Xavier Martinet, Xiaodong Wang, Xiaofang Wang, Xiaoqing Ellen Tan, Xide Xia, Xinfeng Xie, Xuchao Jia, Xuewei Wang, Yaelle Goldschlag, Yashesh Gaur, Yasmine Babaei, Yi Wen, Yiwen Song, Yuchen

Zhang, Yue Li, Yuning Mao, Zacharie Delpierre Coudert, Zheng Yan, Zhengxing Chen, Zoe Papakipos, Aaditya Singh, Aayushi Srivastava, Abha Jain, Adam Kelsey, Adam Shajnfeld, Adithya Gangidi, Adolfo Victoria, Ahuva Goldstand, Ajay Menon, Ajay Sharma, Alex Boesenberg, Alexei Baevski, Allie Feinstein, Amanda Kallet, Amit Sangani, Amos Teo, Anam Yunus, Andrei Lupu, Andres Alvarado, Andrew Caples, Andrew Gu, Andrew Ho, Andrew Poulton, Andrew Ryan, Ankit Ramchandani, Annie Dong, Annie Franco, Anuj Goyal, Aparajita Saraf, Arkabandhu Chowdhury, Ashley Gabriel, Ashwin Bharambe, Assaf Eisenman, Azadeh Yazdan, Beau James, Ben Maurer, Benjamin Leonhardi, Bernie Huang, Beth Loyd, Beto De Paola, Bhargavi Paranjape, Bing Liu, Bo Wu, Boyu Ni, Braden Hancock, Bram Wasti, Brandon Spence, Brani Stojkovic, Brian Gamido, Britt Montalvo, Carl Parker, Carly Burton, Catalina Mejia, Ce Liu, Changhan Wang, Changkyu Kim, Chao Zhou, Chester Hu, Ching-Hsiang Chu, Chris Cai, Chris Tindal, Christoph Feichtenhofer, Cynthia Gao, Damon Civin, Dana Beaty, Daniel Kreymer, Daniel Li, David Adkins, David Xu, Davide Testuggine, Delia David, Devi Parikh, Diana Liskovich, Didem Foss, Dingkang Wang, Duc Le, Dustin Holland, Edward Dowling, Eissa Jamil, Elaine Montgomery, Eleonora Presani, Emily Hahn, Emily Wood, Eric-Tuan Le, Erik Brinkman, Esteban Arcaute, Evan Dunbar, Evan Smothers, Fei Sun, Felix Kreuk, Feng Tian, Filippos Kokkinos, Firat Ozgenel, Francesco Caggioni, Frank Kanayet, Frank Seide, Gabriela Medina Florez, Gabriella Schwarz, Gada Badeer, Georgia Swee, Gil Halpern, Grant Herman, Grigory Sizov, Guangyi, Zhang, Guna Lakshminarayanan, Hakan Inan, Hamid Shojanazeri, Han Zou, Hannah Wang, Hanwen Zha, Haroun Habeeb, Harrison Rudolph, Helen Suk, Henry Aspegren, Hunter Goldman, Hongyuan Zhan, Ibrahim Damlaj, Igor Molybog, Igor Tufanov, Ilias Leontiadis, Irina-Elena Veliche, Itai Gat, Jake Weissman, James Geboski, James Kohli, Janice Lam, Japhet Asher, Jean-Baptiste Gaya, Jeff Marcus, Jeff Tang, Jennifer Chan, Jenny Zhen, Jeremy Reizenstein, Jeremy Teboul, Jessica Zhong, Jian Jin, Jingyi Yang, Joe Cummings, Jon Carvill, Jon Shepard, Jonathan McPhie, Jonathan Torres, Josh Ginsburg, Junjie Wang, Kai Wu, Kam Hou U, Karan Saxena, Kartikay Khandelwal, Katayoun Zand, Kathy Matosich, Kaushik Veeraraghavan, Kelly Michelena, Keqian Li, Kiran Jagadeesh, Kun Huang, Kunal Chawla, Kyle Huang, Lailin Chen, Lakshya Garg, Lavender A, Leandro Silva, Lee Bell, Lei Zhang, Liangpeng Guo, Licheng Yu, Liron Moshkovich, Luca Wehrstedt, Madiam Khabsa, Manav Avalani, Manish Bhatt, Martynas Mankus, Matan Hasson, Matthew Lennie, Matthias Reso, Maxim Groshev, Maxim Naumov, Maya Lathi, Meghan Keneally, Miao Liu, Michael L. Seltzer, Michal Valko, Michelle Restrepo, Mihir Patel, Mik Vyatskov,

Mikayel Samvelyan, Mike Clark, Mike Macey, Mike Wang, Miquel Jubert Hermoso, Mo Metanat, Mohammad Rastegari, Munish Bansal, Nandhini Santhanam, Natascha Parks, Natasha White, Navyata Bawa, Nayan Singhal, Nick Egebo, Nicolas Usunier, Nikhil Mehta, Nikolay Pavlovich Laptev, Ning Dong, Norman Cheng, Oleg Chernoguz, Olivia Hart, Omkar Salpekar, Ozlem Kalinli, Parkin Kent, Parth Parekh, Paul Saab, Pavan Balaji, Pedro Rittner, Philip Bontrager, Pierre Roux, Piotr Dollar, Polina Zvyagina, Prashant Ratanchandani, Pritish Yuvraj, Qian Liang, Rachad Alao, Rachel Rodriguez, Rafi Ayub, Raghotham Murthy, Raghu Nayani, Rahul Mitra, Rangaprabhu Parthasarathy, Raymond Li, Rebekkah Hogan, Robin Battey, Rocky Wang, Russ Howes, Ruty Rinott, Sachin Mehta, Sachin Siby, Sai Jayesh Bondu, Samyak Datta, Sara Chugh, Sara Hunt, Sargun Dhillon, Sasha Sidorov, Satadru Pan, Saurabh Mahajan, Saurabh Verma, Seiji Yamamoto, Sharadha Ramaswamy, Shaun Lindsay, Shaun Lindsay, Sheng Feng, Shenghao Lin, Shengxin Cindy Zha, Shishir Patil, Shiva Shankar, Shuqiang Zhang, Shuqiang Zhang, Sinong Wang, Sneha Agarwal, Soji Sajuyigbe, Soumith Chintala, Stephanie Max, Stephen Chen, Steve Kehoe, Steve Satterfield, Sudarshan Govindaprasad, Sumit Gupta, Summer Deng, Sungmin Cho, Sunny Virk, Suraj Subramanian, Sy Choudhury, Sydney Goldman, Tal Remez, Tamar Glaser, Tamara Best, Thilo Koehler, Thomas Robinson, Tianhe Li, Tianjun Zhang, Tim Matthews, Timothy Chou, Tzook Shaked, Varun Vontimitta, Victoria Ajayi, Victoria Montanez, Vijai Mohan, Vinay Satish Kumar, Vishal Mangla, Vlad Ionescu, Vlad Poenaru, Vlad Tiberiu Mihailescu, Vladimir Ivanov, Wei Li, Wenchen Wang, Wenwen Jiang, Wes Bouaziz, Will Constable, Xiaocheng Tang, Xiaojian Wu, Xiaolan Wang, Xilun Wu, Xinbo Gao, Yaniv Kleinman, Yanjun Chen, Ye Hu, Ye Jia, Ye Qi, Yenda Li, Yilin Zhang, Ying Zhang, Yossi Adi, Youngjin Nam, Yu, Wang, Yu Zhao, Yuchen Hao, Yundi Qian, Yunlu Li, Yuzi He, Zach Rait, Zachary DeVito, Zef Rosnbrick, Zhaoduo Wen, Zhenyu Yang, Zhiwei Zhao, and Zhiyu Ma. The llama 3 herd of models, 2024.

[15] Dan Graur, Damien Aymon, Dan Kluser, Tanguy Albrici, Chandramohan A Thekkath, and Ana Klimovic. Cachew: Machine learning input data processing as a service. In *2022 usenix annual technical conference (usenix atc 22)*, pages 689–706, 2022.

[16] Kaiming He, Xiangyu Zhang, Shaoqing Ren, and Jian Sun. Deep residual learning for image recognition. In *2016 IEEE Conference on Computer Vision and Pattern Recognition (CVPR)*, pages 770–778, 2016.

[17] Michael Isard, Mihai Budiu, Yuan Yu, Andrew Birrell, and Dennis Fetterly. Dryad: distributed data-parallel programs from sequential building blocks. In *Proceedings of the 2nd ACM SIGOPS/EuroSys European conference on computer systems 2007*, pages 59–72, 2007.

[18] Gautier Izacard, Mathilde Caron, Lucas Hosseini, Sebastian Riedel, Piotr Bojanowski, Armand Joulin, and Edouard Grave. Unsupervised dense information retrieval with contrastive learning. *arXiv preprint arXiv:2112.09118*, 2021.

[19] Mandar Joshi, Eunsol Choi, Daniel Weld, and Luke Zettlemoyer. TriviaQA: A large scale distantly supervised challenge dataset for reading comprehension. In Regina Barzilay and Min-Yen Kan, editors, *Proceedings of the 55th Annual Meeting of the Association for Computational Linguistics (Volume 1: Long Papers)*, pages 1601–1611, Vancouver, Canada, July 2017. Association for Computational Linguistics.

[20] Peter Kraft, Daniel Kang, Deepak Narayanan, Shoumik Palkar, Peter Bailis, and Matei Zaharia. Willump: A statistically-aware end-to-end optimizer for machine learning inference. In I. Dhillon, D. Papailiopoulos, and V. Sze, editors, *Proceedings of the 3rd Conference on Machine Learning and Systems (MLSys)*, volume 2, pages 147–159, 2020.

[21] Jay Kreps, Neha Narkhede, Jun Rao, et al. Kafka: A distributed messaging system for log processing. In *Proceedings of the NetDB*, volume 11, pages 1–7. Athens, Greece, 2011.

[22] Woosuk Kwon, Zhuohan Li, Siyuan Zhuang, Ying Sheng, Lianmin Zheng, Cody Hao Yu, Joseph Gonzalez, Hao Zhang, and Ion Stoica. Efficient memory management for large language model serving with page-dattention. In *Proceedings of the 29th Symposium on Operating Systems Principles, SOSP ’23*, page 611–626, New York, NY, USA, 2023. Association for Computing Machinery.

[23] Patrick Lewis, Ethan Perez, Aleksandra Piktus, Fabio Petroni, Vladimir Karpukhin, Naman Goyal, Heinrich Kütter, Mike Lewis, Wen-tau Yih, Tim Rocktäschel, Sebastian Riedel, and Douwe Kiela. Retrieval-augmented generation for knowledge-intensive nlp tasks. In H. Larochelle, M. Ranzato, R. Hadsell, M.F. Balcan, and H. Lin, editors, *Advances in Neural Information Processing Systems*, volume 33, pages 9459–9474. Curran Associates, Inc., 2020.

[24] Frank Sifei Luan, Stephanie Wang, Samyukta Yagati, Sean Kim, Kenneth Lien, Isaac Ong, Tony Hong, Sangbin Cho, Eric Liang, and Ion Stoica. Exoshuffle: An extensible shuffle architecture. In *Proceedings of the ACM SIGCOMM 2023 Conference*, ACM SIGCOMM

'23, page 564–577, New York, NY, USA, 2023. Association for Computing Machinery.

[25] Peter Mattson, Christine Cheng, Cody Coleman, Greg Diamos, Paulius Micikevicius, David Patterson, Hanlin Tang, Gu-Yeon Wei, Peter Bailis, Victor Bittorf, David Brooks, Dehai Chen, Debojoyti Dutta, Udit Gupta, Kim Hazelwood, Andrew Hock, Xinyuan Huang, Atsushi Ike, Bill Jia, Daniel Kang, David Kanter, Naveen Kumar, Jeffery Liao, Guokai Ma, Deepak Narayanan, Tayo Oguntebi, Gennady Pekhimenko, Lillian Pentecost, Vijay Janapa Reddi, Taylor Robie, Tom St. John, Tsuguchika Tabaru, Carole-Jean Wu, Lingjie Xu, Masafumi Yamazaki, Cliff Young, and Matei Zaharia. Mlperf training benchmark. In *Proceedings of the 3rd Conference on Machine Learning and Systems (MLSys)*, volume 2, pages 336–349, Austin, TX, USA, 2020.

[26] Philipp Moritz, Robert Nishihara, Stephanie Wang, Alexey Tumanov, Richard Liaw, Eric Liang, Melih Eli bol, Zongheng Yang, William Paul, Michael I. Jordan, and Ion Stoica. Ray: A distributed framework for emerging AI applications. In *13th USENIX Symposium on Operating Systems Design and Implementation (OSDI 18)*, pages 561–577, Carlsbad, CA, October 2018. USENIX Association.

[27] Derek G Murray, Frank McSherry, Rebecca Isaacs, Michael Isard, Paul Barham, and Martín Abadi. Naiad: a timely dataflow system. In *Proceedings of the Twenty-Fourth ACM Symposium on Operating Systems Principles*, pages 439–455, 2013.

[28] Derek G. Murray, Jiří Šimša, Ana Klimovic, and Ihor Indyk. tf.data: a machine learning data processing framework. *Proc. VLDB Endow.*, 14(12):2945–2958, jul 2021.

[29] Arvind Neelakantan, Tao Xu, Raul Puri, Alec Radford, Jesse Michael Han, Jerry Tworek, Qiming Yuan, Nikolas Tezak, Jong Wook Kim, Chris Hallacy, Johannes Heidecke, Pranav Shyam, Boris Power, Tyna Eloundou Nekoul, Girish Sastry, Gretchen Krueger, David Schnurr, Felipe Petroski Such, Kenny Hsu, Madeleine Thompson, Tabarak Khan, Toki Sherbakov, Joanne Jang, Peter Welinder, and Lilian Weng. Text and code embeddings by contrastive pre-training. *Corr*, abs/2201.10005, 2022.

[30] OpenAI, Josh Achiam, Steven Adler, Sandhini Agarwal, Lama Ahmad, Ilge Akkaya, Florencia Leoni Aleman, Diogo Almeida, Janko Altenschmidt, Sam Altman, Shyamal Anadkat, Red Avila, Igor Babuschkin, Suchir Balaji, Valerie Balcom, Paul Balescu, Haiming Bao, Mohammad Bavarian, Jeff Belgum, Irwan Bello, Jake Berdine, Gabriel Bernadett-Shapiro, Christopher Berner, Lenny Bogdonoff, Oleg Boiko, Madelaine Boyd, Anna Luisa Brakman, Greg Brockman, Tim Brooks, Miles Brundage, Kevin Button, Trevor Cai, Rosie Campbell, Andrew Cann, Brittany Carey, Chelsea Carlson, Rory Carmichael, Brooke Chan, Che Chang, Fotis Chantzis, Derek Chen, Sully Chen, Ruby Chen, Jason Chen, Mark Chen, Ben Chess, Chester Cho, Casey Chu, Hyung Won Chung, Dave Cummings, Jeremiah Currier, Yunxing Dai, Cory Decareaux, Thomas Degry, Noah Deutsch, Damien Deville, Arka Dhar, David Dohan, Steve Dowling, Sheila Dunning, Adrien Ecoffet, Atty Eleti, Tyna Eloundou, David Farhi, Liam Fedus, Niko Felix, Simón Posada Fishman, Juston Forte, Isabella Fulford, Leo Gao, Elie Georges, Christian Gibson, Vik Goel, Tarun Gogineni, Gabriel Goh, Rapha Gontijo-Lopes, Jonathan Gordon, Morgan Grafstein, Scott Gray, Ryan Greene, Joshua Gross, Shixiang Shane Gu, Yafei Guo, Chris Hallacy, Jesse Han, Jeff Harris, Yuchen He, Mike Heaton, Johannes Heidecke, Chris Hesse, Alan Hickey, Wade Hickey, Peter Hoeschele, Brandon Houghton, Kenny Hsu, Shengli Hu, Xin Hu, Joost Huizinga, Shantanu Jain, Shawn Jain, Joanne Jang, Angela Jiang, Roger Jiang, Haozhun Jin, Denny Jin, Shino Jomoto, Billie Jonn, Heewoo Jun, Tomer Kaftan, Łukasz Kaiser, Ali Kamali, Ingmar Kanitscheider, Nitish Shirish Keskar, Tabarak Khan, Logan Kilpatrick, Jong Wook Kim, Christina Kim, Yongjik Kim, Jan Hendrik Kirchner, Jamie Kiros, Matt Knight, Daniel Kokotajlo, Łukasz Kondraciuk, Andrew Kondrich, Aris Konstantinidis, Kyle Kosic, Gretchen Krueger, Vishal Kuo, Michael Lampe, Ikai Lan, Teddy Lee, Jan Leike, Jade Leung, Daniel Levy, Chak Ming Li, Rachel Lim, Molly Lin, Stephanie Lin, Mateusz Litwin, Theresa Lopez, Ryan Lowe, Patricia Lue, Anna Makanju, Kim Malfacini, Sam Manning, Todor Markov, Yaniv Markovski, Bianca Martin, Katie Mayer, Andrew Mayne, Bob McGrew, Scott Mayer McKinney, Christine McLeavey, Paul McMillan, Jake McNeil, David Medina, Aalok Mehta, Jacob Menick, Luke Metz, Andrei Mishchenko, Pamela Mishkin, Vinnie Monaco, Evan Morikawa, Daniel Mossing, Tong Mu, Mira Murati, Oleg Murk, David Mély, Ashvin Nair, Reiichiro Nakano, Rajeev Nayak, Arvind Neelakantan, Richard Ngo, Hyeonwoo Noh, Long Ouyang, Cullen O’Keefe, Jakub Pachocki, Alex Paino, Joe Palermo, Ashley Pantuliano, Giambattista Parascandolo, Joel Parish, Emy Parparita, Alex Passos, Mikhail Pavlov, Andrew Peng, Adam Perelman, Filipe de Avila Belbute Peres, Michael Petrov, Henrique Ponde de Oliveira Pinto, Michael Pokorny, Michelle Pokrass, Vitchyr H. Pong, Tolly Powell, Alethea Power, Boris Power, Elizabeth Proehl, Raul Puri, Alec Radford, Jack Rae, Aditya Ramesh, Cameron Raymond, Francis Real, Kendra Rimbach, Carl Ross, Bob Rotsted, Henri Roussez, Nick Ryder, Mario Saltarelli, Ted Sanders, Shibani Santurkar, Girish Sastry, Heather Schmidt, David Schnurr, John Schulman, Daniel Selsam, Kyla Sheppard, Toki Sherbakov, Jessica

Shieh, Sarah Shoker, Pranav Shyam, Szymon Sidor, Eric Sigler, Maddie Simens, Jordan Sitkin, Katarina Slama, Ian Sohl, Benjamin Sokolowsky, Yang Song, Natalie Staudacher, Felipe Petroski Such, Natalie Summers, Ilya Sutskever, Jie Tang, Nikolas Tezak, Madeleine B. Thompson, Phil Tillet, Amin Tootoonchian, Elizabeth Tseng, Preston Tuggle, Nick Turley, Jerry Tworek, Juan Felipe Cerón Uribe, Andrea Vallone, Arun Vijayvergiya, Chelsea Voss, Carroll Wainwright, Justin Jay Wang, Alvin Wang, Ben Wang, Jonathan Ward, Jason Wei, CJ Weinmann, Akila Welihinda, Peter Welinder, Jia-ayi Weng, Lilian Weng, Matt Wiethoff, Dave Willner, Clemens Winter, Samuel Wolrich, Hannah Wong, Lauren Workman, Sherwin Wu, Jeff Wu, Michael Wu, Kai Xiao, Tao Xu, Sarah Yoo, Kevin Yu, Qiming Yuan, Wojciech Zaremba, Rowan Zellers, Chong Zhang, Marvin Zhang, Shengjia Zhao, Tianhao Zheng, Juntang Zhuang, William Zhuk, and Barret Zoph. Gpt-4 technical report, 2024.

[31] A.K. Parekh and R.G. Gallager. A generalized processor sharing approach to flow control in integrated services networks: the single-node case. *IEEE/ACM Transactions on Networking*, 1(3):344–357, 1993.

[32] Adam Paszke, Sam Gross, Francisco Massa, Adam Lerer, James Bradbury, Gregory Chanan, Trevor Killeen, Zeming Lin, Natalia Gimelshein, Luca Antiga, et al. Pytorch: An imperative style, high-performance deep learning library. *Advances in neural information processing systems*, 32, 2019.

[33] PyTorch. torch.utils.data – pytorch 2.3 documentation, 2024.

[34] Vijay Janapa Reddi, Christine Cheng, David Kanter, Peter Mattson, Guenther Schmuelling, Carole-Jean Wu, Brian Anderson, Maximilien Breughe, Mark Charlebois, William Chou, Ramesh Chukka, Cody Coleman, Sam Davis, Pan Deng, Greg Diamos, Jared Duke, Dave Fick, J. Scott Gardner, Itay Hubara, Sachin Idgunji, Thomas B. Jablin, Jeff Jiao, Tom St. John, Pankaj Kanwar, David Lee, Jeffery Liao, Anton Lokhmotov, Francisco Massa, Peng Meng, Paulius Micikevicius, Colin Osborne, Gennady Pekhimenko, Arun Tejasve Raghunath Rajan, Dilip Sequeira, Ashish Sirasao, Fei Sun, Hanlin Tang, Michael Thomson, Frank Wei, Ephrem Wu, Lingjie Xu, Koichi Yamada, Bing Yu, George Yuan, Aaron Zhong, Peizhao Zhang, and Yuchen Zhou. Mlperf inference benchmark. In *Proceedings of the ACM/IEEE 47th Annual International Symposium on Computer Architecture*, ISCA ’20, page 446–459. IEEE Press, 2020.

[35] Robin Rombach, Andreas Blattmann, Dominik Lorenz, Patrick Esser, and Björn Ommer. High-resolution image synthesis with latent diffusion models. In *Proceedings of the IEEE/CVF Conference on Computer Vision and Pattern Recognition*, pages 10684–10695, 2022.

[36] Yu Sun, Xiaolong Wang, Zhuang Liu, John Miller, Alexei A. Efros, and Moritz Hardt. Test-time training with self-supervision for generalization under distribution shifts. In *Proceedings of the 37th International Conference on Machine Learning*, ICML’20. JMLR.org, 2020.

[37] Gemini Team, Rohan Anil, Sebastian Borgeaud, Yonghui Wu, Jean-Baptiste Alayrac, Jiahui Yu, Radu Soricut, Johan Schalkwyk, Andrew M Dai, Anja Hauth, et al. Gemini: a family of highly capable multimodal models. *arXiv preprint arXiv:2312.11805*, 2023.

[38] Zhan Tong, Yibing Song, Jue Wang, and Limin Wang. Videomae: Masked autoencoders are data-efficient learners for self-supervised video pre-training. In S. Koyejo, S. Mohamed, A. Agarwal, D. Belgrave, K. Cho, and A. Oh, editors, *Advances in Neural Information Processing Systems*, volume 35, pages 10078–10093. Curran Associates, Inc., 2022.

[39] Joseph Torres, Michael Armbrust, Tathagata Das, and Shixiong Zhu. Introducing low-latency continuous processing mode in structured streaming in apache spark 2.3, March 2018.

[40] Shivaram Venkataraman, Aurojit Panda, Kay Ousterhout, Michael Armbrust, Ali Ghodsi, Michael J. Franklin, Benjamin Recht, and Ion Stoica. Drizzle: Fast and adaptable stream processing at scale. In *Proceedings of the 26th Symposium on Operating Systems Principles*, SOSP ’17, page 374–389, New York, NY, USA, 2017. Association for Computing Machinery.

[41] Stephanie Wang, Eric Liang, Edward Oakes, Ben Hindman, Frank Sifei Luan, Audrey Cheng, and Ion Stoica. Ownership: A distributed futures system for {Fine-Grained} tasks. In *18th USENIX Symposium on Networked Systems Design and Implementation (NSDI 21)*, pages 671–686, 2021.

[42] Gyeong-In Yu, Joo Seong Jeong, Geon-Woo Kim, Soo-jeong Kim, and Byung-Gon Chun. Orca: A distributed serving system for {Transformer-Based} generative models. In *16th USENIX Symposium on Operating Systems Design and Implementation (OSDI 22)*, pages 521–538, 2022.

[43] Matei Zaharia, Mosharaf Chowdhury, Michael J Franklin, Scott Shenker, and Ion Stoica. Spark: Cluster computing with working sets. In *2nd USENIX Workshop on Hot Topics in Cloud Computing (HotCloud 10)*, 2010.

- [44] Matei Zaharia, Tathagata Das, Haoyuan Li, Scott Shenker, and Ion Stoica. Discretized streams: an efficient and fault-tolerant model for stream processing on large clusters. In *Proceedings of the 4th USENIX Conference on Hot Topics in Cloud Computing*, HotCloud’12, page 10, USA, 2012. USENIX Association.
- [45] Mark Zhao, Emanuel Adamiak, and Christos Kozyrakis. cedar: Optimized and unified machine learning input data pipelines. *arXiv preprint arXiv:2401.08895*, 2024.
- [46] Yanli Zhao, Andrew Gu, Rohan Varma, Liang Luo, Chien-Chin Huang, Min Xu, Less Wright, Hamid Shojanazeri, Myle Ott, Sam Shleifer, Alban Desmaison, Can Balioglu, Pritam Damania, Bernard Nguyen, Geeta Chauhan, Yuchen Hao, Ajit Mathews, and Shen Li. Pytorch fsdp: Experiences on scaling fully sharded data parallel. *Proc. VLDB Endow.*, 16(12):3848–3860, aug 2023.

A Additional Microbenchmarks

A.1 Fractional Parallelism

In this microbenchmark, we demonstrate that the streaming batch model can maximize the resource utilization when fractional parallelism is required. Consider a two-stage data pipeline, in which the first stage takes 1 second on average, and the second stage takes 2 seconds. Ideally, the operator parallelisms should be set as 2 : 1 to balance the throughput. In traditional stream processing systems such as Flink, this is unattainable on a 8-CPU machine, because it requires setting the operator parallelisms to be 2.67 and 5.33, respectively. Since these systems allocate executors to operators statically, they cannot support fractional parallelism. In contrast, the streaming batch execution model allows Ray Data to multiplex executors for both stages dynamically during run time. The Ray Data scheduler can dynamically start a task for either stage in order to balance the throughput, effectively achieving a parallelism ratio of 2 : 1 over time. [Figure 11](#) shows that when comparing to a static allocation of 4–4 executors for each stage, the dynamic allocation increases the utilization of the execution slots, manifested as fewer bubbles in the schedule, and 19% faster job completion time.

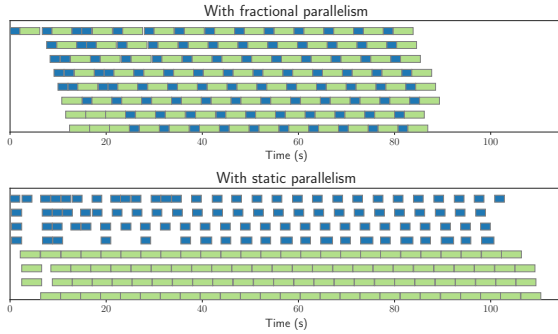


Figure 11: Dynamically allocated executor slots can achieve fractional parallelism with better resource utilization (fewer bubbles).

B Solver for Discrete-time Scheduling

To verify the efficacy of the online scheduling algorithm, we develop a discrete-time simulation environment, in which tasks have fixed execution times, and a discrete-time solver that can find the optimal schedule to run a data pipeline, subject to specified resource constraints.

The input to the solver is a data pipeline, the total data size, and the resource constraints. The data pipeline is described as a chain of operators. Each operator processes data in tasks. Each task has an input size and an output size measured in number of partitions, and we assume each task has a known duration. Each task also has a resource requirement, e.g. 1 CPU or 1 GPU.

The total data size is also measured in number of partitions. The resource constraints describe how many execution slots are available for each resource type (CPU or GPU), and also

has a memory buffer limit, indicating how many intermediate partitions in total can be stored in the temporary memory buffer.

Finally, the solver has a length limit, measured in time ticks, for any solution returned. This is such that the solution space is bounded.

B.1 Algorithm

The solution space is defined by the set of all possible execution states. The execution state consists of:

- Time since the start.
- The state of each executor, i.e. which operator task is running.
- The state of the shared memory buffer, which is the number of partitions stored in the buffer.
- The state of each operator, which is the number of pending tasks.

The solver starts from the initial state (time 0, all executors idle, buffer empty, and all tasks pending). For each state, it generates the next state by emulating the execution: advancing the tick, updating executor states, updating the progress of running tasks, updating the memory buffer, etc. The number of next states is determined by the size of the set of all possible scheduling actions, which is the power set of all possible scheduling *primitives*. A scheduling primitive would be “schedule the next task operator i onto executor j .”

The solver runs a variation of the A* search algorithm to try to arrive at the first completion state (in which no more tasks are pending). In the priority queue, the states are sorted by the number of completed tasks, i.e. it prioritizes states that make further progress. The solver returns the optimal job completion time after all possible states are visited.

The naive search algorithm is not practical due to its high time complexity ($O((E \cdot T)^N)$), where N is the total number of tasks, E the total number of executors, and T the time limit). We use the following optimizations to bring the complexity down to $O(2^N \cdot T)$, making it more practical for large scheduling problems.

- Symmetry of tasks and executors. We assign a canonical ordering of the executors, i.e. the first task always starts on the lowest-numbered executor. This gets rid of a large class of duplicate states, where the task timings are the same, except that they run on different executors.
- Temporal equivalence. We notice that the optimal job completion time given an execution state at time t is the same, regardless of its execution history before t . This means all states that arrive at the same task progress at time t are equivalent. This is crucial for reducing the number of duplicate states, and in many cases, reduces the problem to polynomial time.

For the scheduling microbenchmark in [Section 5.3.1](#), the solver finds the optimal schedule with a total run time of 153 seconds.